UDC 629.735.33
DOI: 10.15587/2706-5448.2024.298600

**Valentyn Pelykh,**
**Volodymyr Andryushchenko**

# DETERMINATION OF THE FEATURES OF INTEGRATED DESIGNING OF CIVIL LONG-RANGE AIRCRAFT WITH TRANSONIC TRUSS-BRACED WING AT THE PRELIMINARY DESIGN STAGE

*The object of research is a civil mainline aircraft with a transonic truss-braced wing. The problem of designing an aircraft of this scheme at the preliminary design stage is being solved in the work. The results of the work include the concept of designing aircraft with a transonic truss-braced wing, the main advantages of such a scheme, the process of determining the geometric parameters of the truss-braced, features of the preliminary design of an aircraft with an extremely high aspect ratio truss-braced wing, possible approaches to the arrangement of units and their mutual arrangement. The results are explained by the difference in the design model (the cantilever beam is replaced by a beam on two supports) in mass analysis and the increased wing aspect ratio in aerodynamic calculation. The final data are based on a statistical study to determine the basic geometric parameters of assemblies of modern mainline passenger aircraft, synthesis of parameters of analog aircraft. For example, an aircraft capable of carrying 250 passengers over a distance of 13.000 km is considered. In the design process, values of aspect ratio, taper ratio, wing area, vertical tail and horizontal tail area ratio, and fuselage dimensions are accepted. Drawings of the general appearance of the aircraft have been developed and, based on it, a master geometry of the theoretical contour has been constructed. Graphs of first-order polar and maximum lift-to-drag ratio have been plotted, the reduction of aerodynamic drag in percentage terms has been determined, and the increase in aerodynamic lift-to-drag ratio in percentage terms for an aircraft with an extremely high aspect ratio truss-braced wing compared to similar characteristics of an aircraft with a conventional non-braced wing has been calculated. The approximate mass savings when using a truss-braced wing on the aircraft are determined in percentage terms. The expediency of using wings of greater aspect ratio, than modern aircraft currently have, has been justified. The expediency of using a brace for the aircraft with an extremely high aspect ratio wing has been justified. The obtained results can be used in practice in the process of developing the preliminary design of an aircraft with a truss-braced wing or in the modifications of existing aircraft to increase their fuel efficiency or increase the durability of wing elements due to reduced loads acting on them.*

**Keywords:** *mainline aircraft, truss-brace, zero approximation, preliminary design, master geometry, statistical study, aerodynamic efficiency and mass efficiency.*

*Received date: 23.12.2023*
*Accepted date: 14.02.2024*
*Published date: 21.02.2024*



***How to cite***
*Pelykh, V., Andryushchenko, V. (2024). Determination of the features of integrated design of civil long-range aircraft with transonic truss-braced wing at the preliminary design stage. Technology Audit and Production Reserves, 1 (1 (75)), 35–42. doi: https://doi.org/10.15587/2706-5448.2024.298600*

## 1. Introduction

TTBW (Transonic Truss-Braced Wing) is an innovative design under investigation for use in modern aircraft to reduce resistance during flight [1]. This work examines the basic principles of TTBW construction and the advantages of its application in aircraft.

The high aspect ratio wing with struts shaped as aerodynamic profiles is one of the main elements of TTBW technology [2]. The wings of modern airliners have aspect ratios of approximately 9–12. This aspect ratio ensures the presence of a sufficiently large inductive resistance during flight, leading to increased fuel consumption and reduced flight range.

Aerodynamic braces (AB) relieve the wing from bending moments, allowing for an increase in its span due to an extremely high aspect ratio [3–5], which can reach 20–30. The larger is a span, the less is inductive resistance.

The main advantage of TTBW construction is the reduction of drag during flight. This allows aircraft to reduce fuel consumption, increase flight range, and reduce $CO_2$ emissions [6]. Additionally, TTBW technology allows for increased flight speed and reduced noise, which is particularly important in airports. Another advantage of TTBW construction is the improvement of aircraft stability and control. Boeing and NASA are currently the main developers of this technology.

ISSN 2664-9969

All these advantages enhance operational efficiency [7]. By reducing fuel consumption and increasing flight range, operating costs can be lowered and profitability increased.

At the layout development stage and the aerodynamic braces' scheme selection, it is considered necessary to introduce certain limitations in the aircraft design process:

– since the strut is intended to create a reaction at the attachment point, it is advisable to direct it in a way that the strut stretches during flight, leading to the selection of the «wing-body» configuration, i. e. high-wing configuration;
– to move the horizontal tail (HT) out of the wake region, it is advisable to select the T-shaped «HT-fuselage» configuration;
– the placement of engines is chosen based on two opposing requirements. If placed behind the aerodynamic brace, a noise shield effect is achieved. However, if they are mounted on pylons under the wing between the fuselage and the aerodynamic brace, wing loading during flight and parking can be facilitated, resulting in a lighter wing;
– the strut should be integrated with the fuselage structure in a way that reduces the number of reinforced frames. This can be achieved by structurally shaping it into the landing gear well contour (in a high-wing configuration it will be placed in the fuselage) with the same frames that carry loads from the wing.

All other aircraft parameters can be considered separately because the configuration envisages a fundamentally new wing structure, and other components do not require significant configuration changes, as demonstrated by Boeing and NASA, which plan to retrofit existing aircraft to the new scheme.

An interesting issue is the placement of fuel tanks. The required wing area remains unchanged, but the volume of the wing box decreases due to the increased aspect ratio. This limits the volume of tanks that can be located in the wing. The placement issue is resolved by utilizing the internal space of the struts and fuselage. Additionally, Boeing and NASA have claimed fuel savings of up to 10–15 % in TTBW-equipped aircraft, which reduces the required volume of fuel tanks.

During the stages of developing the load-carrying structure (LCS), attention should be paid to the methods of wing and strut attachment. Several attachment zones can be distinguished – wing-to-fuselage, wing-to-strut, strut-to-fuselage. The joints of these elements can be either moment-bearing or moment-free. If hinge joints are installed at all points, the structure becomes statically determinate. This approach was adopted in this work, as it facilitates calculations.

However, if a statically indeterminate structure is chosen, the wing calculation is considered appropriate to be conducted using force method. At the preliminary design stage, the stiffness values of the wing and strut are unknown. One possible solution is to specify a single stiffness value and the stiffness ratio between the elements, and to solve the problem using classical methods of structural mechanics.

This scheme does not impose restrictions on the LCS of the wing, but the most optimal solution, based on the criterion of minimum mass, would be to align wings and struts with identical layouts [8].

High aspect ratio wings will have a larger span, increasing proportionally to the square root of the aspect ratio increase. To ensure possible operation of such aircraft at lower class airports, concepts involving wingtip folding mechanisms during landing exist [9].

*The aim of the research* is to develop recommendations for shaping the external appearance, arrangement, and positioning of aircraft components for the designed aircraft, as well as their alignment. This will enable a more thorough approach to the development of the preliminary design of an aircraft with a high aspect ratio braced wing. To achieve this, the following steps are necessary:

– To determine the influence of a high aspect ratio braced wing shaped as airfoil on the aerodynamic and mass characteristics of aircraft.
– To analyze of the efficiency of using high aspect ratio braced wings on aircraft.
– To quantitatively compare the indicators of aircraft designed under identical requirements with high aspect ratio truss-braced wings and conventional non-braced wings.
– To assess the influence of wing aspect ratio on the performance specifications of the aircraft.

## 2. Materials and Methods

For an aircraft with a high aspect ratio truss-braced wing, it is currently impossible to find direct analogs. The only solution may be to use small aircraft, such as Cessna series planes, as analogs for aircraft with conventional braces. For large commercial passenger aircraft, aircraft not provided with braces can be used as analogs, but values such as sweep angle, aspect ratio, and wingspan should not be used as statistical data. Instead, the values of the dimensions of the high aspect ratio wing should be set within certain reasonable ranges at this stage and adjusted iteratively as the aircraft design calculations progress.

In this work, the following requirements for the performance specifications (PS) of the aircraft are proposed: maximum speed $V_{\max} = 920$ km/h, maximum altitude $H_{\max} = 12000$ m, cruising speed $V_{cr} = 900$ km/h, maximum range with maximum fuel reserve $L_{\max m_f} = 13000$ km and maximum payload $L_{\max m_{pl}} = 8000$ km correspondingly, and payload mass $m_{pl} = 25000$ kg, passenger capacity $n_p = 250$ people.

Based on the developed requirements specification (RS), 5 analog aircraft have been selected that meet the stated requirements and are already in operation in the airline industry. Statistical data reflecting the current level of aircraft manufacturing and available mass, geometric, and PS of the aircraft in use have been collected and processed using the methodology outlined in the sources [10, 11].

The following analog aircraft have been chosen:

– Airbus A350 XWB;
– Airbus A340-200;
– Boeing 777-200LR;
– Boeing 787-9;
– Airbus A330-200.

All aircraft parameters are assumed to be average or close to average, within the ranges of the analog aircraft values. Wing and brace parameters were independently determined based on the works [1–9]. The main PS and parameters of the assemblies are listed in Tables 1, 2.

For the aircraft under design, a braced airfoil attached to the fuselage lower part and the wing lower surface has been selected. The main parameters for this aircraft are: the relative coordinate to the wing console attachment ($\bar{Z}_{tb}$), the relative coordinate to the aircraft fuselage attachment ($\bar{X}_{fa}$), the root ($b_{0tb}$) and tip ($b_{ktb}$) chords of the brace.

**Table 1**

Performances

| $M_{H_{cr}}$ | $M_{max}$ | $L_{max\,m_{pl}}$, km | $L_{max\,m_f}$, km | $n_p$, people | $L_t$, m | $L_l$, m | $H_{max}$, m | $H_{cr.}$, m | $n_{cr.m}$, persons |
|---|---|---|---|---|---|---|---|---|---|
| 0.846 | 0.865 | 8000 | 13000 | 250 | 3000 | 2600 | 12000 | 11000 | 10 |

**Notes:** $M_{(H_{cr}=11\,km)}$ – Mach number at cruising altitude; $M_{max}$ – maximum Mach number; $L_t$ and $L_l$ – length of take-off run and landing run, respectively; $H_{cr}$ – cruise altitude; $n_{cr.m}$ – number of crew members

**Table 2**

Main parameters of aircraft truss-braced assemblies

| $\lambda_{wing}$ | $\chi_{wing}$, ° | $\eta_{wing}$ | $\bar{c}$ | $\bar{S}_{ai}$ | $\lambda_f$ | $D_f$, m | $L_f$, m | $\eta_{VT}$ |
|---|---|---|---|---|---|---|---|---|
| 22 | 11 | 2.5 | 0.14 | 0.04 | 10 | 5.97 | 61.9 | 1 |
| $\bar{S}_{HT}$ | $\bar{S}_{VT}$ | $\lambda_{HT}$ | $\lambda_{VT}$ | $\chi_{HT}$, ° | $\chi_{VT}$, ° | $\bar{c}_{HT}$ | $\bar{c}_{VT}$ | $\eta_{HT}$ |
| 0.23 | 0.18 | 4.9 | 1.25 | 25 | 40 | 0.12 | 0.12 | 3.25 |

**Notes:** $\lambda_{wing}$, $\lambda_{HT}$, $\lambda_{VT}$, $\lambda_f$ – aspect ratio of the wing, horizontal tail (HT), vertical tail (VT), and fuselage; $\eta_{wing}$, $\eta_{VT}$, $\eta_{HT}$ – wing taper ratio, VT taper ratio, and HT taper ratio; $\chi_{wing}$, $\chi_{HT}$, $\chi_{VT}$ – sweep angle at the leading edge of the wing, HT, and VT; $D_f$, $L_f$ – fuselage diameter and length; $\bar{S}_{ai}$, $\bar{S}_{HT}$, $\bar{S}_{VT}$ – ailerons, HT, VT areas' ratio; $\bar{c}$, $\bar{c}_{HT}$, $\bar{c}_{VT}$ – wing, HT and VT profiles thicknesses' ratio

According to the developments of NASA and Boeing [9] it is assigned that, $\bar{Z}_{nk} = 0.5$, then:

$$Z_{tb} = \bar{Z}_{tb} \cdot \frac{l}{2} = 0.5 \cdot \frac{93.5}{2} = 23.375 \text{ m},$$

where $Z_{tb}$ – distance from the fuselage axis to the point of brace-to-wing attachment, m; $l$ – wingspan of the aircraft, m.

The relative brace-to-fuselage attachment coordinate is selected based on the following condition:

$$\bar{X}_{sc} < \bar{X}_{tbf} \le \bar{X}_{wt},$$

where $\bar{X}_{SC}$ – relative coordinate of the wing's center of stiffness (in zero approximation, its position is assumed to be along the 0.25 chord line of the airfoil); $\bar{X}$ – relative coordinate of the airfoil tip.

It is accepted in the zero approximation $\bar{X}_{tbf} = \bar{X}_{wt}$.

The central chord of the brace $(b_{0tb})$ is adopted based on NASA work [9]:

$$b_{0tb} = 2.82 \text{ m}.$$

The taper ratio of the aerodynamic strut $(\eta_{tb})$ 2, is adopted, then:

$$b_{ktb} = \frac{b_{0tb}}{\eta_{tb}} = \frac{2.82}{2} = 1.41 \text{ m}.$$

Based on this data, drawings of the general view (Fig. 1) and the master-geometry of the aircraft (Fig. 2) were constructed.

In Fig. 1, three projections of the aircraft are depicted. Illuminators, emergency exits, and hatches are marked on the fuselage. Controls and high lift devices are shown on the aerodynamic surfaces, as well as the mean aerodynamic chord.

Fig. 2 represents a surface model created according to the drawing shown in Fig. 1 and is subsequently used as a theoretical contour in aerodynamics calculations and for the construction of individual aircraft elements.

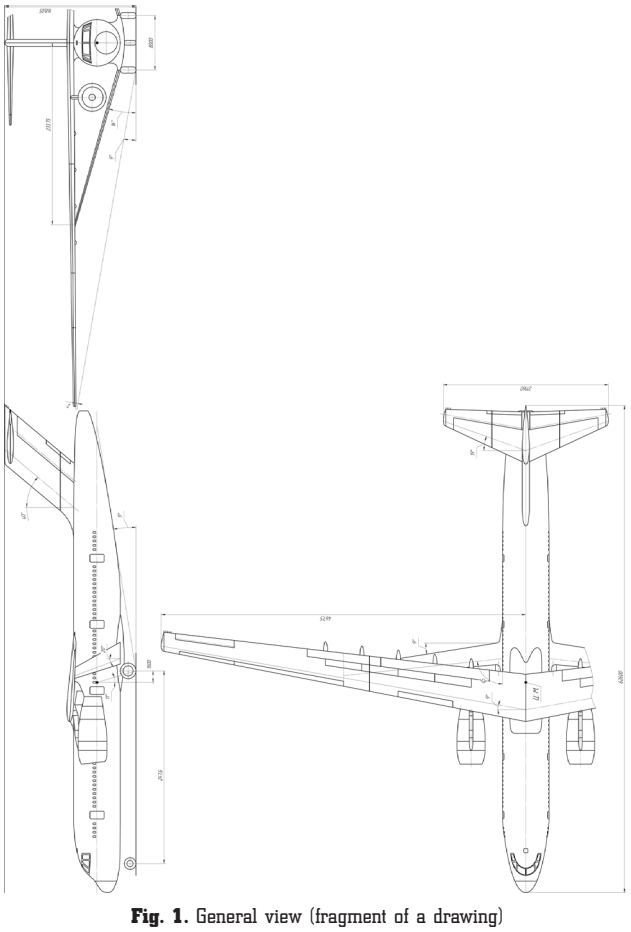

**Fig. 1.** General view (fragment of a drawing)

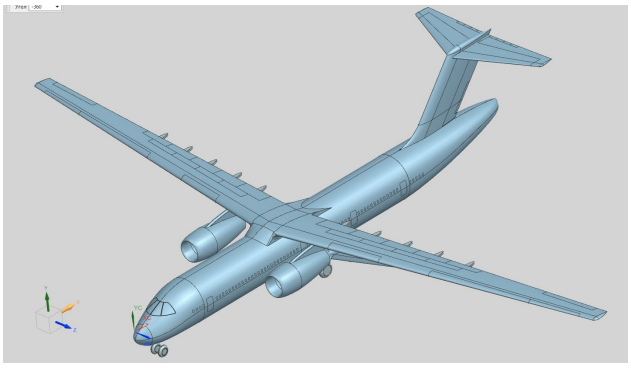

**Fig. 2.** Master-geometry of the plane

## 3. Results and Discussion

One of the main claimed advantages of aircraft with high aspect ratio braced wings is the reduction of the drag, which was determined in this study using two methods: analytical and FEM.

The analytical method is based on the work [12]. Using software developed at the Department of Aircraft Designing

ISSN 2664-9969

of the National Aerospace University «Kharkiv Aviation Institute» (Ukraine), the calculations were performed for aircraft (option 1 with high aspect ratio wings $\lambda_{wing} = 22$, option 2 – with normal aspect ratio wings $\lambda_{wing} = 10$), the parameters of which are listed in Tables 2 and 3.

**Table 3**

The main parameters of aircraft non-braced units

| $\lambda_{wing}$ | $\chi_{wing}$, ° | $\eta_{wing}$ | $\bar{c}$ | $\bar{S}_{ai}$ | $\lambda_f$ | $D_f$, m | $L_f$, m | $\eta_{VT}$ |
|---|---|---|---|---|---|---|---|---|
| 10 | 11 | 2.5 | 0.14 | 0.04 | 10 | 5.97 | 61.9 | 1 |
| $\bar{S}_{HT}$ | $\bar{S}_{VT}$ | $\lambda_{HT}$ | $\lambda_{VT}$ | $\chi_{HT}$, ° | $\chi_{VT}$, ° | $\bar{c}_{HT}$ | $\bar{c}_{VT}$ | $\eta_{HT}$ |
| 0.23 | 0.18 | 4.9 | 1.25 | 25 | 40 | 0.12 | 0.12 | 3.25 |

The change in wing aspect ratio necessitates a recalculation of the wing span, as well as the tip and root chords. The aircraft configurations for aerodynamic analysis are depicted in Fig. 3.

The results of the aerodynamic calculations are presented in Tables 4, 5.

The results presented in Tables 4, 5 can be interpreted in the form of two graphs (Fig. 4, 5).

The numerical calculation was performed using the finite difference method in the Ansys CFX software package [13]. For the calculation, isolated surfaces of the wing and braced wing of the respective aircraft variants were constructed (Fig. 6, 7).

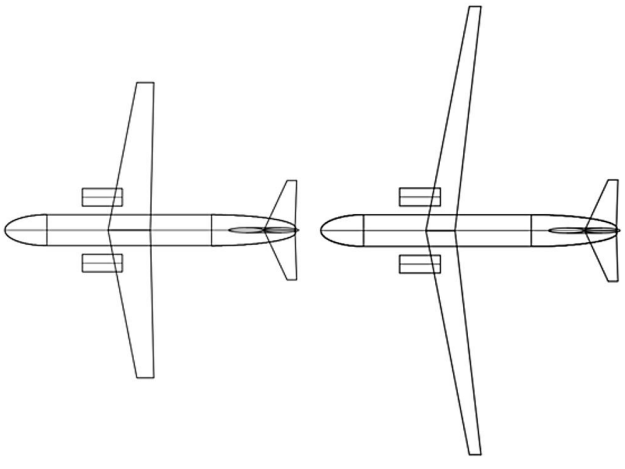

**Fig. 3.** Comparative configurations of aircraft with conventional and high aspect ratio wings

**Table 4**

The polar diagram of the aircraft $C_{xa}$ with aerodynamic brace (option 1)

| Parameter | $M = 0.2$ | $M = 0.3$ | $M = 0.4$ | $M = 0.5$ | $M = 0.6$ | $M = 0.7$ | $M = 0.8$ |
|---|---|---|---|---|---|---|---|
| $C_{ya} = 0.0$ | 0.01849 | 0.01799 | 0.01767 | 0.01744 | 0.01726 | 0.0171 | 0.01696 |
| $C_{ya} = 0.2$ | 0.0192 | 0.01871 | 0.0184 | 0.01817 | 0.01799 | 0.01784 | 0.0177 |
| $C_{ya} = 0.4$ | 0.02149 | 0.02102 | 0.02073 | 0.02054 | 0.02039 | 0.02028 | 0.0202 |
| $C_{ya} = 0.6$ | 0.02558 | 0.02517 | 0.02496 | 0.02486 | 0.02483 | 0.02486 | 0.02495 |
| $C_{ya} = 0.8$ | 0.03176 | 0.0315 | 0.03148 | 0.03162 | 0.03188 | 0.03229 | 0.03289 |
| $C_{ya} = 1.0$ | 0.04062 | 0.04073 | 0.04119 | 0.04196 | 0.04313 | 0.04492 | 0.06923 |
| $C_{ya} = 1.2$ | 0.05396 | 0.05545 | 0.05829 | 0.06545 | – | – | – |
| $C_{ya} = \max$ | 0.08926 | 0.08688 | 0.08466 | 0.08251 | 0.08039 | 0.0903 | 0.10703 |
| $K_{\max}$ | 25.234 | 25.403 | 25.41 | 25.318 | 25.152 | 24.923 | 24.636 |

**Table 5**

The polar diagram of the aircraft $C_{xa}$ without aerodynamic brace (option 2)

| Parameter | $M = 0.2$ | $M = 0.3$ | $M = 0.4$ | $M = 0.5$ | $M = 0.6$ | $M = 0.7$ | $M = 0.8$ |
|---|---|---|---|---|---|---|---|
| $C_{ya} = 0.0$ | 0.01827 | 0.01777 | 0.01746 | 0.01724 | 0.01706 | 0.0169 | 0.01676 |
| $C_{ya} = 0.2$ | 0.01977 | 0.01927 | 0.01896 | 0.01874 | 0.01857 | 0.01842 | 0.01828 |
| $C_{ya} = 0.4$ | 0.0244 | 0.02392 | 0.02364 | 0.02345 | 0.02331 | 0.0232 | 0.02311 |
| $C_{ya} = 0.6$ | 0.03238 | 0.03197 | 0.03176 | 0.03166 | 0.03163 | 0.03165 | 0.03173 |
| $C_{ya} = 0.8$ | 0.04402 | 0.04376 | 0.04373 | 0.04385 | 0.04411 | 0.0445 | 0.04506 |
| $C_{ya} = 1.0$ | 0.05987 | 0.05997 | 0.06041 | 0.06116 | 0.06229 | 0.064 | 0.09291 |
| $C_{ya} = 1.2$ | 0.08169 | 0.08311 | 0.0858 | 0.09217 | – | – | – |
| $C_{ya} = \max$ | 0.12456 | 0.12004 | 0.11564 | 0.11129 | 0.10696 | 0.11814 | 0.13647 |
| $K_{\max}$ | 18.609 | 18.816 | 18.92 | 18.967 | 18.976 | 18.956 | 18.914 |

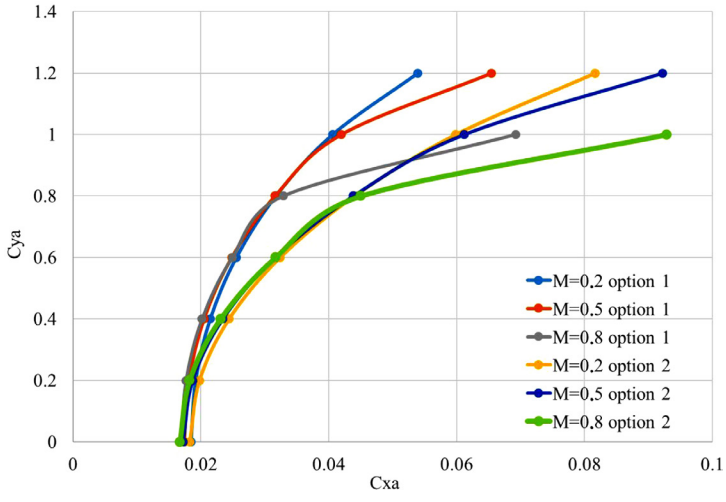


**Fig. 4.** Polar plots of the first kind for two aircraft configurations

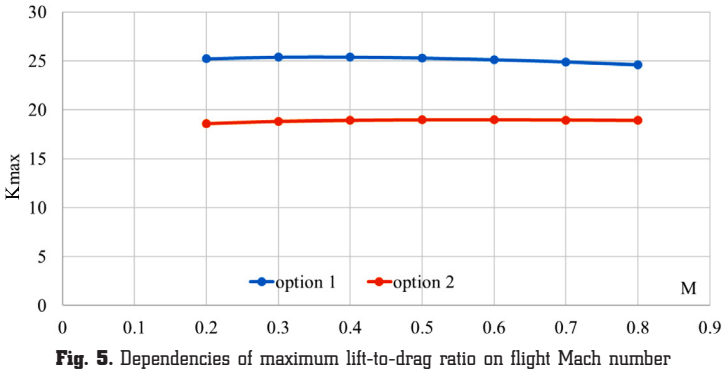


**Fig. 5.** Dependencies of maximum lift-to-drag ratio on flight Mach number for two aircraft configurations

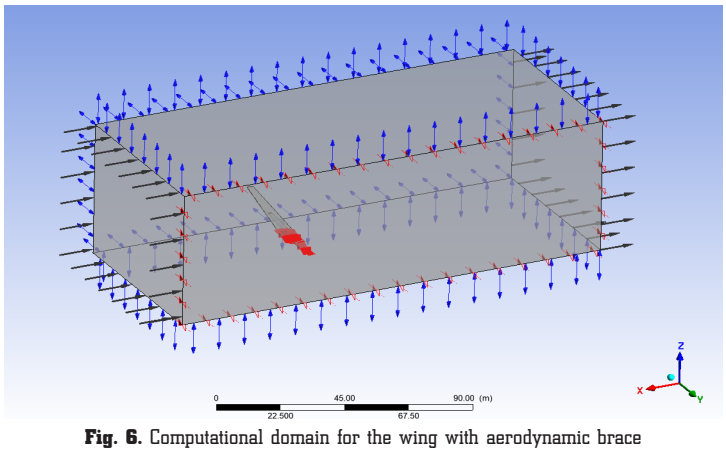

**Fig. 6.** Computational domain for the wing with aerodynamic brace

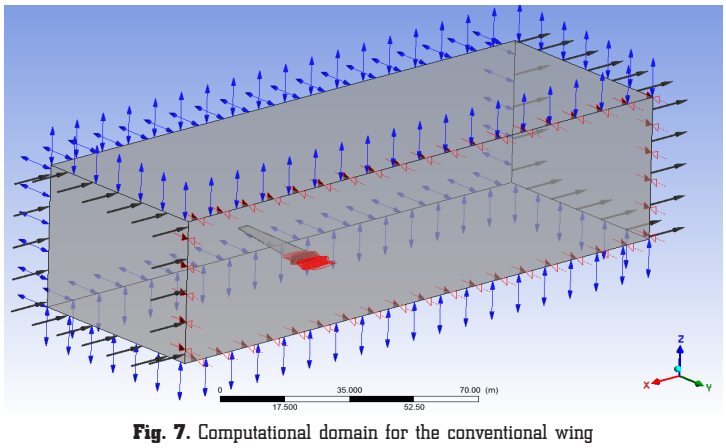

**Fig. 7.** Computational domain for the conventional wing

The aerodynamic efficiency was determined as a combination of factors, including the ratio of lift forces, drag forces, lift-to-drag ratio, and losses due to the vortices of two isolated wings: a high aspect ratio wing with aerodynamic strut (option 1) and a conventional wing (option 2).

The computational domain represented a volume of air with a cutout portion corresponding to the models of the two wings. The boundary conditions were as follows:

– airspeed at the inlet – 900 km/h;
– excessive pressure at the outlet – 0 Pa;
– open zones with excessive pressure – 0 Pa;
– symmetry condition along the wing's edge;
– wall conditions.

The calculation results are listed in Table 6.

**Table 6**

The results of aerodynamic calculations

| Parameter | Option 1 | Option 2 | Dimensionality | Relative change |
|---|---|---|---|---|
| Lift force | 3782090 | 2698000 | N | 28.66 % |
| Drag force | 373378 | 300867 | N | 19.42 % |
| Lift-to-drag ratio | 10.129 | 8.967 | – | 11.47 % |

The pressure distribution is shown in Fig. 8, 9.

As seen from Table 6, the absolute values of lift force and drag force with the same airfoil, twist, and wing area have been increased. This can be primarily explained by the fact that the losses due to air flow from lower pressure areas to higher pressure areas depend on the wing's aspect ratio. The increase in drag force is attributed to imperfections in the geometry of the wing-strut system.

The wingtips were not considered in the calculation, as such an analysis would become multiparametric, making it more difficult to determine the effectiveness of the high aspect ratio wing.

The indicator of the effectiveness of the chosen solution is the lift-to-drag ratio, which increased by 11.47 % for the isolated wing, from 8.967 to 10.129, indicating the validity of the decision made.

The increase in the aircraft's lift-to-drag ratio can have several positive consequences:

– *fuel savings*. Increasing the lift-to-drag ratio can help reduce fuel consumption by lowering the inductive air resistance;
– *speed enhancement*. Decreasing air resistance can also help increase the aircraft's maximum speed;
– *increased maximum flight altitude*. Improving the lift-to-drag ratio can contribute to raising the aircraft's maximum flight altitude, which can be useful for avoiding adverse weather conditions or other air hazards;
– *extended flight range*. More efficient engine operation due to reduced air resistance can extend the aircraft's flight range on a single refueling;
– *improved maneuverability*. Increasing the aerodynamic quality can enhance the aircraft's angle of attack, allowing it to fly without losing stability, enabling more complex maneuvers and maneuvering in confined spaces.

ISSN 2664-9969

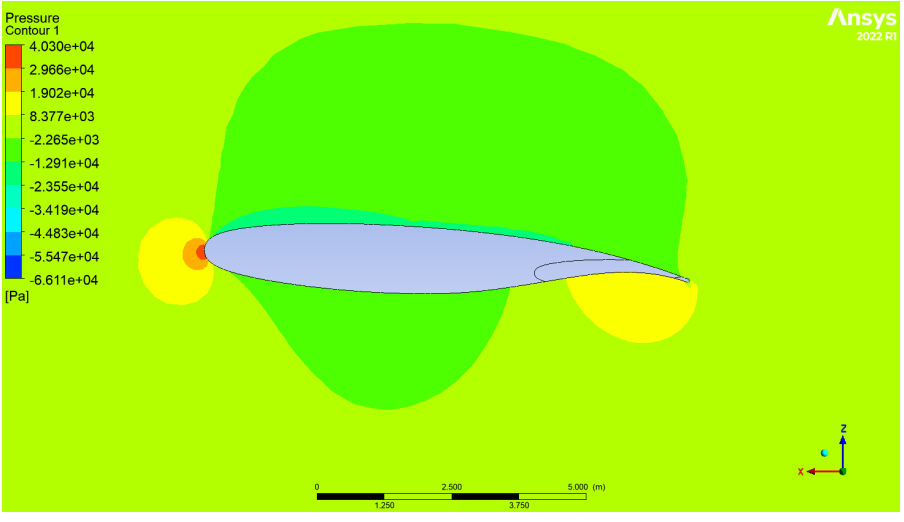


**Fig. 8.** Pressure distribution for the isolated wing of the conventional scheme

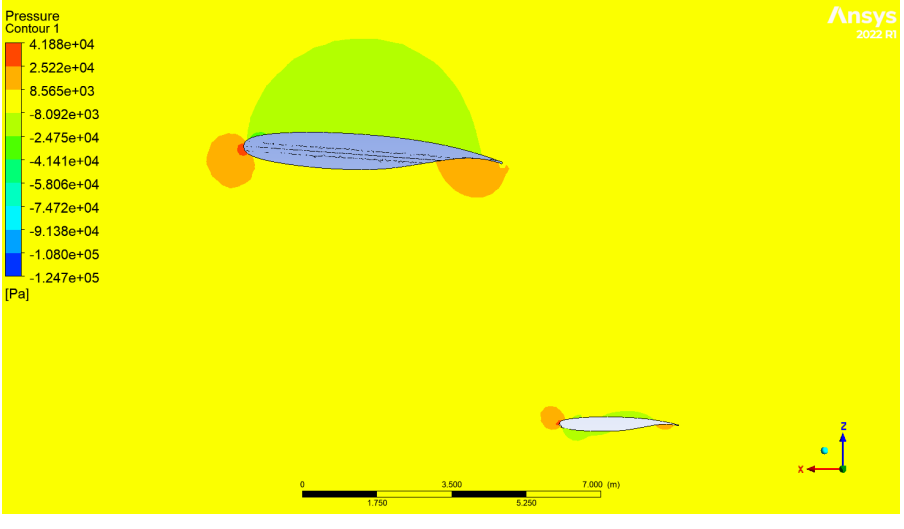


**Fig. 9.** Pressure distribution for the isolated truss-braced wing

Overall, enhancing the lift-to-drag ratio of the aircraft can improve its economic and technical characteristics, provide greater flight safety, and make it more efficient in accomplishing tasks.

In the preliminary stage of determining the aircraft parameters, three design options have been considered:

1) With a high aspect ratio wing with aerodynamic bracing (option 1);

2) With a high aspect ratio wing without aerodynamic bracing (option 2);

3) With a conventional wing without bracing (option 3).

A method for evaluating the mass efficiency of this design has been considered.

The mass of the aircraft wing depends on the dimensions and quantity of transverse and longitudinal load-bearing elements. According to the criterion of minimum mass, the dimensions of all load-bearing elements are determined under the condition of equilibrium and failure at maximum calculated loads.

Thus, the weight of the wing is proportional to the load acting on it. To assess the load, longitudinal ($N$) and transverse ($Q$) force diagrams, bending ($M_x$) and torsional ($M_z$) moment diagrams spanwise are used (Fig. 10–13). The methodology for constructing these diagrams is provided in references [14–18].

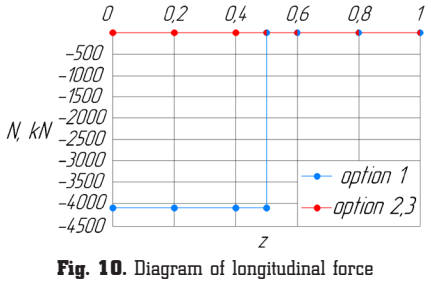


**Fig. 10.** Diagram of longitudinal force

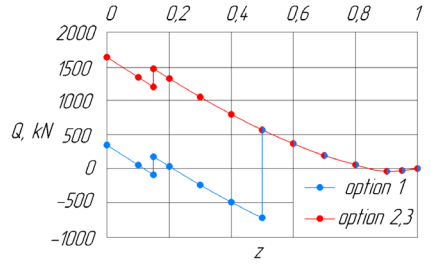


**Fig. 11.** Diagram of transverse force

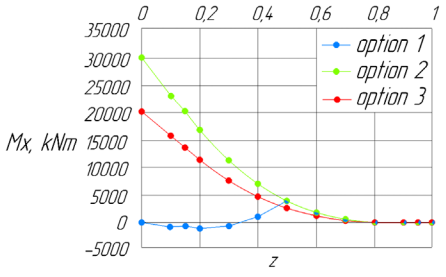


**Fig. 12.** Diagram of bending moment

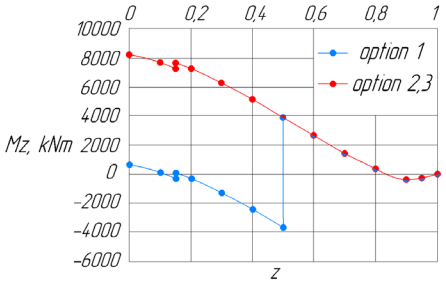


**Fig. 13.** Diagram of torsional moment

Analyzing diagrams, the following conclusions were drawn:
– Longitudinal force arises only in the braced wing;
– Internal force factors in the braced wing are times less than in wings without braces;
– In the selected scheme, the brace is tensed, while the wing under the brace is compressed.

It should be noted that the high aspect ratio wing has a larger span, so the diagrams in relative coordinates should be adjusted according to the wingspan.

For analysis (according to [15]), averaged parameters across the wing span were used:

$$N_{av} = \sum_{i=1}^{n} N_i / n = \left| \begin{matrix} 2174026\ \text{N} \\ j=1 \end{matrix} \right| \left| \begin{matrix} 0\ \text{N} \\ j=2 \end{matrix} \right| \left| \begin{matrix} 0\ \text{N} \\ j=3 \end{matrix} \right|;$$

$$M_{x\,av} = \sum_{i=1}^{n} M_{x,i} / n =$$

$$= \left| \begin{matrix} 1027032\ \text{N}\cdot\text{m} \\ j=1 \end{matrix} \right| \left| \begin{matrix} 9309101\ \text{N}\cdot\text{m} \\ j=2 \end{matrix} \right| \left| \begin{matrix} 6279645\ \text{N}\cdot\text{m} \\ j=3 \end{matrix} \right|,$$

where $N_{av}$ – average longitudinal force, N; $M_{x\,av}$ – average bending moment, N·m; $n$ – number of calculated sections; $j$ – variant number of wing construction; $i$ – number of the $i$-th calculated section.

Since compression is only carried by the wing of variant 1, it is convenient to consider it in the calculation of bending moments as a preloading factor.

The dimensions of the wing elements are selected based on the value of the bending moment. For this purpose, the following calculation sequence from reference [15] is used:

$$G_M = G_{M`} + G_{N`} + G_N;$$

$$G_N = l_{tb} \cdot f_{\min} \cdot \rho = l_{tb} \cdot \frac{S}{\sigma_B} \cdot \rho = 20.65 \cdot \frac{4274784}{\sigma_B} \cdot \rho = \frac{88274289 \cdot \rho}{\sigma_B};$$

$$G_{M`} = \frac{l}{2} \cdot f_{\min} \cdot \rho = \frac{l}{2} \cdot \frac{M_{x\,av}}{\sigma_B \cdot b \cdot \bar{c}} \cdot \rho;$$

$$G_{M`1} = \frac{93.5}{2} \cdot \frac{1027032}{\sigma_B \cdot 4.51 \cdot \bar{c}} \cdot \rho = \frac{10646063 \cdot \rho}{\sigma_B \cdot \bar{c}} = \frac{76043307 \cdot \rho}{\sigma_B};$$

$$G_{M`2} = \frac{93.5}{2} \cdot \frac{9309101}{\sigma_B \cdot 4.51 \cdot \bar{c}} \cdot \rho = \frac{96496778 \cdot \rho}{\sigma_B \cdot \bar{c}} = \frac{689262700 \cdot \rho}{\sigma_B};$$

$$G_{M`3} = \frac{63}{2} \cdot \frac{6279645}{\sigma_B \cdot 6.63 \cdot \bar{c}} \cdot \rho = \frac{29835417 \cdot \rho}{\sigma_B \cdot \bar{c}} = \frac{213110121 \cdot \rho}{\sigma_B};$$

$$G_{N`} = \frac{l}{2} \cdot f_{\min} \cdot \rho = \frac{l}{2} \cdot \frac{N_{av}}{\sigma_B \cdot b_A} \cdot \rho = \frac{93.5}{2} \cdot \frac{2174026}{\sigma_B \cdot 4.51} \cdot \rho =$$

$$= \frac{22535635 \cdot \rho}{\sigma_B};$$

$$G_{M1} = G_{M`1} + G_{N`} + G_N = \frac{186853231 \cdot \rho}{\sigma_B};$$

$$G_{M2} = G_{M`2} = \frac{689262700 \cdot \rho}{\sigma_B};$$

$$G_{M`3} = \frac{213110121 \cdot \rho}{\sigma_B},$$

where $S$ – wing area, m$^2$; $f_{\min}$ – minimum required area of longitudinal load-bearing elements, m$^2$; $\sigma_B$ – material ultimate strength of load-bearing elements, MPa; ρ – density of load-bearing material, kg/m$^3$; $b_A$ – mean aerodynamic chord of the wing (MAC), m; $l_{tb}$ – length of the brace, m; $G_M$ – calculated mass of wing longitudinal load-bearing elements subjected to bending, kg; $G_{M`}$ – calculated mass of wing longitudinal load-bearing elements subjected to pure bending, kg; $G_{N`}$ – calculated mass of wing longitudinal load-bearing elements subjected to tension-compression, kg; $G_N$ – calculated mass of strut longitudinal load-bearing elements subjected to tension-compression, kg.

As seen from the calculations, the mass of one truss-braced wing (TBW) console (option 1) is 14 % less than the mass of one console of a conventional wing (option 3). The mass of the high aspect ratio wing without bracing (option 2) will be 3–4 times more than the other options.

The aerodynamic results can be explained by the fact that with increasing aspect ratio, the structural efficiency inevitably increases, leading to improved fuel efficiency and financial savings.

The weight results can be explained by the fact that the calculated configuration of the braced wing is a beam on two supports, while the calculated configuration of the cantilever wing is a cantilevered beam. With the same loading, the first configuration yields significantly lower bending moments, making the structure lighter.

The practical significance of the study lies in determining specific values of aerodynamic and mass efficiency of the aircraft with different types of wings. Subsequently, when assessing all characteristics, a decision can be made to develop a new wide-body aircraft with such a wing configuration.

The limitation of the study lies in the accuracy of the calculations. It is recommended to repeat them on more precise models using powerful servers or in the process of conducting physical experiments.

In wartime conditions, the study was conducted using numerical methods without physical experiments in wind tunnels.

Prospectively, it is worth investigating the influence of various geometric parameters of the wing and bracing on aerodynamic and mass characteristics, as well as studying the peculiarities of aeroelastic phenomena in the new design. A separate issue is ensuring the resource of the wing-to-brace and fuselage-to-brace joints.

ISSN 2664-9969

## 4. Conclusions

During this study, the main features of integrated designing for civil passenger aircraft with an aerodynamic brace configuration have been determined:

– The layout peculiarities of the main aircraft components when using the TTWB scheme have been identified;

– Proposals have been provided to address potential issues in the arrangement of aircraft systems (fuel system, takeoff and landing system);

– Justification of the aerodynamic efficiency of using high aspect ratio wings compared to wings of the conventional scheme has been presented;

– A method for determining the weight efficiency of the braced wing configuration compared to the wing of the conventional scheme has been proposed.

Based on the aerodynamic calculations and analysis, it was found that an aircraft designed using statistical data and employing the TTWB wing configuration has approximately 10–20 % higher lift-to-drag ratio (depending on flight Mach number and lift force generated) and lower aerodynamic drag compared to a conventional lower aspect ratio wing without braces. This correlates with the demands of aerospace companies for a 10–15 % reduction in fuel consumption.

The mass efficiency calculation determined that:

– the average bending moment for a braced wing is six times smaller than that for a conventional wing;

– the total mass of the «wing + braces» structure is 14 % less than the mass of a standard classical wing (with equal other parameters);

– the use of a high aspect ratio wing without braces at this development stage is not advisable because the bending moment on the wing (and hence its mass) increases disproportionately more than the lift-to-drag ratio of the structure;

– the brace should be located under the wing, hence the preferable configuration for an aircraft with braces is a high-wing configuration, as in this case, the brace will stretch under load in flight and thus will not lose stability.

## Conflict of interest

The authors declare that they have no conflict of interest in relation to this study, whether financial, personal, authorship or otherwise, that could affect the study and its results presented in this paper.

## Financing

The research was performed without financial support.

## Data availability

The manuscript has no associated data.

## Use of artificial intelligence

The authors confirm that they did not use artificial intelligence technologies when creating the current work.

### References

1. Ting, E., Reynolds, K. W., Nguyen, N. T., Totah, J. (2014). Aerodynamic Analysis of the Truss-Braced Wing Aircraft Using Vortex-Lattice Superposition Approach. *32nd AIAA Applied Aerodynamics Conference*. Atlanta, Reston. doi: https://doi.org/10.2514/6.2014-2597
2. Allen, T., Sexton, B., Scott, M. J. (2015). SUGAR Truss Braced Wing Full Scale Aeroelastic Analysis and Dynamically Scaled Wind Tunnel Model Development. *56th AIAA/ASCE/AHS/ASC Structures, Structural Dynamics, and Materials Conference*. Kissimmee, Reston. doi: https://doi.org/10.2514/6.2015-1171
3. Gur, O., Bhatia, M., Mason, W. H., Schetz, J. A., Kapania, R. K., Nam, T. (2011). Development of a framework for truss-braced wing conceptual MDO. *Structural and Multidisciplinary Optimization, 44 (2)*, 277–298. doi: https://doi.org/10.1007/s00158-010-0612-9
4. Harrison, N. A., Gatlin, G. M., Viken, S. A., Beyar, M., Dickey, E. D., Hoffman, K., Reichenbach, E. Y. (2020). Development of an Efficient M=0.80 Transonic Truss-Braced Wing Aircraft. *AIAA Scitech 2020 Forum*. Orlando, Reston. doi: https://doi.org/10.2514/6.2020-0011
5. Gur, O., Bhatia, M., Mason, W., Schetz, J., Kapania, R., Nam, T. (2010). Development of Framework for Truss-Braced Wing Conceptual MDO. *51st AIAA/ASME/ASCE/AHS/ASC Structures, Structural Dynamics, and Materials Conference 18th AIAA/ASME/AHS Adaptive Structures Conference 12th*. Orlando, Reston. doi: https://doi.org/10.2514/6.2010-2754
6. Hosseini, S., Ali Vaziri-Zanjani, M., Reza Ovesy, H. (2020). Conceptual design and analysis of an affordable truss-braced wing regional jet aircraft. *Proceedings of the Institution of Mechanical Engineers, Part G: Journal of Aerospace Engineering*. doi: https://doi.org/10.1177/0954410020923060
7. Lee, K., Nam, T., Kang, S. (2017). Propulsion System Modeling and Reduction for Conceptual Truss-Braced Wing Aircraft Design. *International Journal of Aeronautical and Space Sciences, 18 (4)*, 651–661. doi: https://doi.org/10.5139/ijass.2017.18.4.651
8. Ting, E., Chaparro, D., Nguyen, N. T. (2017). Development of an Integrated Nonlinear Aeroservoelastic Flight Dynamic Model of the Truss-Braced Wing Aircraft. *58th AIAA/ASCE/AHS/ASC Structures, Structural Dynamics, and Materials Conference*. Grapevine, Reston. doi: https://doi.org/10.2514/6.2017-1815
9. Wells, D. P. (2017). Cruise Speed Sensitivity Study for Transonic Truss Braced Wing. *55th AIAA Aerospace Sciences Meeting*. Grapevine, Reston. doi: https://doi.org/10.2514/6.2017-1628
10. Mialitca, A. K., Malashenko, L. A., Grebenikov, A. G. et al. (2010). *Razrabotka avanproekta samoleta*. Kharkiv: Natc. aerokosm. un-t «Khark. aviatc. in-t», 233.
11. Poliakov, V. S., Andryushchenko, V. M., Topal, M. S. (2024). *Vyznachennia parametriv litaka v nulovomu nablyzhenni*. Kharkiv: Nats. aerokosm. un-t «Kharkiv. aviats. in-t», 201.
12. Eremenko, S. M. (2019). *Aerodinamika letatelnykh apparatov*. Kharkiv: Natc. aerokosm. un-t im. N. E. Zhukovskogo «Kharkiv. aviatc. in-t», 384.
13. Fedorova, N. N., Valger, S. A., Danilov, M. N., Zakharova, Iu. V. (2017). *Osnovy raboty v ANSYS 17*. DMK Press, 210.
14. *Raschet kryla samoleta na staticheskuiu prochnost i zhestkost* (2009). GOUVPO «KnAGTU», 90.
15. Voit, E. S., Endogur, A. I., Melik-Sarkisian, Z. A., Aliavdin, I. M. (1987). *Proektirovanie konstruktcii samoletov*. Mashinostroenie, 416.
16. Evseev, L. A. (1985). *Raschet na prochnost kryla bolshogo udlineniia*. Kharkiv: Khark. aviatc. in-t, 106.
17. Fomichev, P. A., Zarutckii, A. V., Mandziuk, S. F. (2017). *Raschet na prochnost samoleta. Ch. 1*. Kharkov: Natc. aerokosm. un-t im. N. E. Zhukovskogo «Kharkiv. aviatc. in-t», 165.
18. Chepurnykh, I. V. (2013). *Prochnost konstruktcii letatelnykh apparatov*. FGBOU VPO «KnAGTU», 137.

✉ ***Valentyn Pelykh,*** *Postgraduate Student, Department of Aircraft Designing, National Aerospace University «Kharkiv Aviation Institute», Kharkiv, Ukraine; Design Engineer, Department of Strength, State Concern «Motor-Sich», DB named after I. Sikorskyi, Zaporizhzhia, Ukraine; Lecturer, Department of Aircraft Design Disciplines, Zaporizhzhia Aviation Vocational College named after O. H. Ivchenko, Zaporizhzhia, Ukraine, e-mail: venator.verba@gmail.com, ORCID: https://orcid.org/0009-0007-5301-6697*

***Volodymyr Andryushchenko,*** *Senior Researcher, PhD, Associate Professor, Department of Aircraft Designing, National Aerospace University «Kharkiv Aviation Institute», Kharkiv, Ukraine, ORCID: https://orcid.org/0000-0003-1013-3803*

✉ *Corresponding author*